Electrochimica Acta 55 (2010) 8638–8648

Contents lists available at ScienceDirect

Electrochimica Acta

journal homepage: www.elsevier.com/locate/electacta

Simultaneous voltammetric determination of acetaminophen, aspirin and caffeine using an in situ surfactant-modified multiwalled carbon nanotube paste electrode

Bankim J. Sanghavi, Ashwini K. Srivastava*

Department of Chemistry, University of Mumbai, Vidyanagari, Santacruz (East), Mumbai 400 098, India

ARTICLE INFO

Article history:
Received 13 May 2010
Received in revised form 27 July 2010
Accepted 29 July 2010
Available online 6 August 2010

Keywords:
Acetaminophen
Aspirin
Caffeine
Carbon nanotubes
Triton X 100

ABSTRACT

A carbon nanotube paste electrode modified in situ with Triton X 100 was developed for the individual and simultaneous determination of acetaminophen (ACOP), aspirin (ASA) and caffeine (CF). The electrochemical behavior of these three molecules was investigated employing cyclic voltammetry (CV), electrochemical impedance spectroscopy (EIS), chronocoulometry (CC) and adsorptive stripping differential pulse voltammetry (AdSDPV). Kramers–Kronig transformation implied that the resulting impedance data were validated and were of very good quality. These studies revealed that the oxidation of ACOP, ASA and CF is facilitated at an in situ surfactant-modified multiwalled carbon nanotube paste electrode (ISSM-CNT-PE). After optimization of analytical conditions employing this electrode at pH 7.0 in phosphate buffer (0.1 M), the peak currents for the three molecules were found to vary linearly with their concentrations in the range of 2.91×10^{-7}–6.27×10^{-5} M with detection limits of 2.58×10^{-8}, 8.47×10^{-8} and 8.83×10^{-8} M for ACOP, ASA and CF respectively using AdSDPV. The prepared modified electrode showed several advantages, such as a simple preparation method, high sensitivity, very low detection limits and excellent reproducibility. Furthermore, the proposed method was employed for the simultaneous determination of ACOP, ASA and CF in pharmaceutical formulations, urine and blood serum samples and the obtained results were found to be satisfactory.

1. Introduction

Combination drugs consisting of acetaminophen (ACOP), aspirin (ASA) and caffeine (CF) are used to treat pain from conditions such as headache (including migraine), muscle aches, menstrual cramps, arthritis, backache, toothaches, colds and sinus infections. However, an overdose of these combination drugs may induce nausea, vomiting, diarrhea, abdominal pain, sweating, seizures, confusion or an irregular heartbeat. Hence, their determination in trace quantities is of great importance. Previously, electrochemical techniques have been implemented for the estimation of ACOP [1–6], ASA [7–9] and CF [10–14] when present individually. Other instrumental techniques employed for the individual analysis of three molecules are: HPLC–MS/MS, GC–MS/MS, spectrofluorimetry for ACOP [15–17], UV–vis spectrophotometry, solid-phase fluorescence spectroscopy for ASA [18–20] and GC–MS, micellar electrokinetic capillary chromatography, Quasi-flow injection analysis for CF [21–23]. However, there are relatively few methods for their simultaneous estimation [24–27]. Moreover, these methods face the drawbacks of being expensive, laborious and requiring pretreatment of the samples. Surprisingly, no voltammetric procedure exists for the simultaneous determination of ACOP, ASA and CF in a mixture. Therefore, it is desirable to develop simple, sensitive and precise alternate methods employing carbon paste electrodes for the simultaneous determination of all three molecules.

Carbon paste electrodes (CPEs) are very popular due to their wide anodic potential range, low residual current, ease of fabrication, easy surface renewal and low cost. Chemically modified electrodes (CMEs) are used to lower the detection limits compared to plain carbon paste electrodes (PCPE). Various modifiers, such as macrocyclic compounds [28,29], copper complexes [30,31], phthalocyanine [32] and nanomaterials [33] have been employed successfully as modifiers for carbon paste electrodes. Carbon nanotubes (CNTs) have triggered a new genre for the development of novel electrode materials due to their amazing structural, mechanical, electrical and physical properties [34–38]. In addition, surfactants at trace levels have also been employed successfully as modifiers [39–43].

In view of the desirable characteristics of CNTs and surfactants, it is likely that electrochemical processes may occur in

* Corresponding author. Fax: +91 022 26528547.
E-mail addresses: aksrivastava@chem.mu.ac.in, akschbu@yahoo.com (A.K. Srivastava).

0013-4686/$ – see front matter © 2010 Elsevier Ltd. All rights reserved.
doi:10.1016/j.electacta.2010.07.093

a facile manner on surfactant-CNT modified carbon paste electrodes. Therefore, the present work aims to employ adsorptive stripping differential pulse voltammetry (AdSDPV) for the individual and simultaneous determination of ACOP, ASA and CF at an in situ surfactant-modified multiwalled carbon nanotube paste electrode (ISSM-CNT-PE). The surface characterization of these electrodes is performed using a scanning electron microscope (SEM). The electrochemical characterizations of the obtained electrodes have been carried out through cyclic voltammetry (CV), electrochemical impedance spectroscopy (EIS) and chronocoulometry (CC). Utilizing the developed method, individual and simultaneous determination of the three molecules has been carried out in pharmaceutical formulations, urine and blood serum samples. Additionally, CF was successfully analyzed in beverages, coffee and cola. Moreover, the proposed voltammetric method was validated by UV–vis spectrophotometry for ACOP, potentiometry for CF and titrimetry for ASA.

2. Experimental

2.1. Chemicals and instrumentation

All chemicals were of A.R. grade and were used as received without any further purification. ACOP, ASA, CF, ascorbic acid, D-glucose, uric acid, NaH_2PO_4 and Na_2HPO_4 were purchased from S.D. Fine (India). Urea and 4-aminophenol were procured from Loba Chemie (India). MWCNTs (dimensions: OD = 60–100 nm, ID = 5–10 nm, length = 0.5–50 μm, C 95+%) were obtained from Aldrich (USA). Graphite powder was purchased from S.D. Fine (India). Mineral oil was purchased from Fluka (USA). Sodium lauryl sulfate (SLS), Triton X 100 (TX 100), cetyl trimethylammonium bromide (CTAB), cetyl pyridinium chloride (CPC), Tween 20, Tween 80, Brij 35 and Brij 56 were purchased from S.D. Fine (India). All solutions were prepared using double distilled water of specific conductance (0.3–0.8 μS).

All voltammetric measurements were performed on an Eco Chemie, Electrochemical Work Station, model Autolab PGSTAT 30 (The Netherlands) having the GPES software (version 4.9.005). All pH measurements were performed using an ELICO LI 120 pH meter. A Ag/AgCl electrode and a platinum electrode were used as the reference and counter electrodes respectively. All potentials were measured with respect to Ag/AgCl(aq) (3 M KCl) as the reference electrode. A plain carbon paste electrode (PCPE), carbon nanotube paste electrode (CNT-PE), an in situ surfactant-modified paste electrode (ISSM-PE) and an in situ surfactant-modified carbon nanotube paste electrode (ISSM-CNT-PE) were used as working electrodes. The UV–vis spectrophotometer used for validating the method was obtained from Shimadzu (Japan). The scanning electron microscope employed for surface characterization of the electrodes was a FEI Quanta-200 model with an operating voltage of 20 kV.

2.2. Preparation of the PCPE, CNT-PE and ISSM electrodes

The PCPE was prepared using slurry composed of 70:30, graphite:mineral oil, using a mortar and pestle, which was then allowed to homogenize for 48 h. The paste was then filled into a Teflon micropipette tip (diameter = 0.5 mm). A metallic wire was dissected through the paste thus providing the electrical contact. Smooth and fresh electrode surfaces were obtained by squeezing out 0.5 mm of paste from the syringe, scraping off the excess and polishing it against butter paper until the surface had a shiny appearance. The CNT-PE was prepared in the same way as the PCPE, but with a composition of 65:5:30, graphite:CNT:mineral oil. For the pretreatment of CNTs, 0.05 g of carbon nanotubes was dispersed in 60 mL of 2.2 M HNO_3 for 20 h at room temperature with the aid of ultrasonic agitation, then washed with distilled water to neutrality and dried in an oven at 37 °C [44]. In situ modification of the electrode was done by dipping the PCPE and the CNT-PE in vigorously stirred (at 400 rpm) surfactant (TX 100) solution for 120 s. These modified electrodes were then dipped in standard ACOP, ASA and CF solutions containing 5×10^{-5} M TX 100 during measurements.

2.3. The treatment and determination of samples

For stripping voltammetric analysis of ACOP, ASA and CF, appropriate quantities of the analyte solution was placed into a 25 mL standard volumetric flask and then diluted to the mark with phosphate buffer, pH 7.0 (0.1 M). The solution was then transferred into the micro-electrochemical cell where the measurements were carried out. A magnetic stirrer (Expo Hi-Tech, India) with a stirring bar was used to provide the convective transport of the analyte during its accumulation onto the carbon paste electrode surface. An accumulation potential of −0.7 V was applied to the ISSM-CNT-PE for an accumulation duration of 300 s while the solution was stirred at 400 rpm with the magnetic stirrer. At the end of the accumulation period, the stirring was stopped, and a 15 s rest period was allowed for the solution to become quiescent. The voltammogram was then recorded by scanning the potential towards the positive direction from −0.1 V to +1.5 V for all three analytes present together using the differential pulse mode employing a step potential of 5 mV and a modulation amplitude of 50 mV. Similarly, cyclic voltammetric experiments were carried out by scanning the potential from −0.4 V to +1.7 V for all three molecules when present together at a scan rate of 10 mV s^{-1}. Double potential step chronocoulometry was carried out with a pulse period of 5 s from +0.3 V to +0.7 V for ACOP, +0.6 V to +1.0 V for ASA and +1.1 V to +1.6 V for CF vs. Ag/AgCl.

Individual analysis of ACOP, ASA and CF was first carried out in pharmaceutical formulations. For simultaneous determination of ACOP, ASA and CF, Cipstrong tablet (Cipla Ltd., India) and two synthetic samples were employed. Twenty tablets of ACOP (and ASA) were weighed and ground to a fine powder using a mortar and pestle. In all the samples where ASA was present, the weighed amount of the powder was boiled with 0.01 N NaOH for 10 min, thus hydrolyzing it completely into salicylic acid [45,46]. The amount of salicylic acid obtained was then equated to the original amount of ASA in the samples. Different beverage samples viz., espresso and instant coffee samples along with two samples of cola beverages were then analyzed for their CF content. The cola samples were appropriately diluted (1:200) with supporting electrolyte to bring them into the working range. Similar treatment was also given to the coffee-based samples. Furthermore, caffeine-free cola sample and a decaffeinated coffee samples were also analyzed with the aim of testing the contribution of the matrix to the analyte signal. The caffeine contents of these samples were almost zero. For all of these experiments, the samples were diluted to 100 mL with pH 7.0 phosphate buffer solution.

Recovery tests were performed for simultaneous determination by spiking standard solutions of all three molecules into pharmaceutical formulations as well as urine and blood serum samples from healthy volunteers. Human blood serum samples were obtained from a local pathology clinic and stored under refrigeration. To avoid interferences of the serum matrix, a 50-μL serum sample was added to the electrochemical cell containing 25 mL of pH 7.0 phosphate buffer solution having 5×10^{-5} M of TX 100. These samples were cleaned by filtering through a 0.22-μm PVDF syringe filter (Millex, Millipore Corporation) with no prior extraction steps before voltammetric measurements.

3. Results and discussion

3.1. Effect of pH and supporting electrolyte

Standard solutions of ACOP, ASA and CF (2×10^{-6} M) were used to find the optimum pH of the supporting electrolyte best suited for determination of ACOP, ASA and CF by PCPE. The influence of the pH on the oxidation peaks currents of ACOP, ASA and CF were investigated in the pH range of 2–12 employing Britton–Robinson buffer. It was observed that as the pH of the medium was gradually increased, the potential shifted towards less positive values, suggesting the involvement of protons in the reaction. At very low pH values, ACOP was hydrolyzed to p-aminophenol. As the pH increased beyond 7.0, however, the peak current decreased and above pH 8.0, there is a distortion in the peak shape. Furthermore, as the pH was increased above 8.0 the oxidation became kinetically less favorable, presumably due to the presence of the phenoxide. Over the pH range 5.5–8.0, the peak potential (E_p) was a linear function of pH for all three molecules. From the plot of E_p vs. pH, slopes of −0.063 V, −0.030 V and −0.065 V were obtained for ACOP (Fig. S1), ASA and CF respectively in the working pH range. This result revealed that an equal number of protons and electrons were involved in the oxidation reactions of ACOP and CF, whereas an unequal number was involved in the oxidation of ASA. It was also observed that the peak current (i_p) reached its maximum value at pH 7.0 for ACOP, ASA and CF oxidation. Thus, this pH was employed for further studies. Various buffers, such as Tris, citrate phosphate, HEPES and phosphate buffer were then employed at pH 7.0 (Fig. S2). Out of these buffers, the pH 7.0 phosphate buffer gave the best response in terms of peak current and peak shape and, hence, was employed for all future experiments. In the next step, optimization of buffer concentration was carried out by varying its concentration in the range of 0.02–0.2 M. The best peak response was observed for 0.1 M phosphate buffer and therefore used for all further studies.

3.2. Effect of CNTs and different surfactants on the oxidation peaks of ACOP, ASA and CF

The effect of the amount of CNTs as a modifier in the carbon paste was first studied by varying its composition in the range of 1–10% with respect to graphite. It was then observed that the oxidation peak current for ACOP, ASA and CF increased with increases in the percentage of CNTs up to 5%; beyond this point, saturation in the anodic peak current occurred. As a result, 5% CNTs was selected as the optimum amount for the preparation of the CNT-PE.

The effects on the peak current of ACOP, ASA and CF were investigated using the following: cationic surfactants, such as CTAB, CPC and CPB; anionic surfactants, such as SLS; and non-ionic surfactants, such as Tween 20, Tween 80, Brij 56, Brij 35 and TX 100. It should be highlighted here that ACOP (pK_a = 9.5, M.W. = 151.16) is a neutral molecule at neutral pH. Therefore, upon employing cationic surfactants, its oxidation peak disappeared and its determination was impossible. Conversely, cationic surfactants enhanced the peak current for ASA (pK_a = 3.5, M.W. = 180.16) and CF (pK_a = 0.7, M.W. = 194.19). In the presence of anionic surfactants, however, the peaks for ASA and CF were not observed.

Based on these observations, conditions conducive for the simultaneous determination of ACOP, ASA and CF were yet to be selected. It was observed that on employing non-ionic surfactants, however, that the peak current for all three molecules increased drastically. Among all the non-ionic surfactants, TX 100 gave the best response in terms of peak current for all three molecules of interest and, hence, was employed for further studies.

The oxidation peak currents of ACOP, ASA and CF were observed to be highly dependent on the concentration of TX 100 and the nature of the electrode. While gradually increasing the concentration of TX 100 from 1×10^{-7} M, the oxidation peak current initially increased up to a concentration of 5×10^{-5} M and then leveled off till 2.8×10^{-4} M due to surface saturation. Beyond this concentration, the peak current intensity started to decrease (Fig. S3) due to the micelle effect. Hence, TX 100 was employed at what was deemed the best concentration of 5×10^{-5} M, well below the CMC (3×10^{-4} M) of TX 100. The observed increase in peak current could be attributed to the TX 100, which has hydrophobic C–H chains and hydrophilic head groups that adsorb strongly at the surface of the carbon paste via hydrophobic interactions. Consequently, adsorbed TX 100 induced ACOP, ASA and CF adsorbtion on to the electrode surface. Therefore, the oxidation current of ACOP, ASA and CF increased significantly in the presence of TX 100. Moreover, ACOP, ASA and CF were solubilized by TX 100, increasing their residence time near the electrode (i.e., TX-100 forms a thin layer on the electrode surface into which the analyte molecules are preconcentrated). This phenomenon then increased the probability of electron transfer between the electrode and all three molecules. As a result, the oxidation peak potentials shifted to less positive values due to induced and associated adsorption [47].

3.3. Scanning electron microscope (SEM)

Fig. 1 compares the morphological features of the different electrodes using SEM. The SEM profile of PCPE was characterized by a surface of irregularly shaped graphite particles that appeared to remain isolated (Fig. 1(a)). The SEM image of ISSM-PE, however, was more uniform in nature: no separated graphite particles could be observed, which demonstrates the good adherence of the surfactant to the graphite (Fig. 1(b)). Furthermore, the SEM image of ISSM-CNT-PE, having CNT at the centre [the rod-like structure at the center of the Fig. 1(c)], with a coating of surfactant was more compact in comparison to PCPE. Hence, the current increases at the ISSM-CNT-PE could be attributed to the more compact nature of the carbon paste due to surfactant and an increased surface area due to MWCNTs.

3.4. Cyclic voltammetry (CV)

The cyclic voltammograms of ACOP, ASA and CF (1×10^{-6} M) at all four investigated electrodes are given in Fig. 2. It can be observed from Fig. 2(a) that moving from PCPE to ISSM-CNT-PE, the anodic and cathodic peak potentials of ACOP shifted towards less positive and less negative values respectively. Thus, the separation in peak potential (ΔE_p) value decreased drastically, indicating that the rate of electrode reaction increased with surfactant modification. At a scan rate of 10 mV s^{-1}, the electrode reaction became reversible with a formal potential of $E_0^1 = 0.30$ V. As shown in Fig. 2(b) and (c), the E_p values for ASA and CF shifted by −100 mV and −30 mV, respectively, in the anodic range. This result implied that the oxidation of all three molecules become facile on the ISSM-CNT-PE.

The effect of potential scan rate on the peak current of ACOP, ASA and CF was also simultaneously studied. Fig. 2(d) shows that ACOP gave a quasireversible cyclic voltammogram, while ASA and CF were completely irreversible in nature. From Fig. 2(d), it can be seen that the oxidation peak shifted to a more positive value for ACOP, ASA and CF, and the reduction peak for ACOP shifted to more negative values with increasing scan rates that had concurrent increases in current. The cyclic voltammetric results indicated that the anodic peak currents (i_p) of the three molecules varied linearly with the scan rate (ν) in the range from 100 mV s^{-1} to 3500 mV s^{-1}. This finding implied that the oxidation of ACOP, ASA and CF was kinetically controlled on the ISSM-CNT-PE.

3.5. Electrochemical impedance spectroscopy (EIS)

In an attempt to clarify the differences among the electrochemical performance of the PCPE, the ISSM-PE, the CNT-PE and the ISSM-CNT-PE, electrochemical impedance spectroscopy (EIS) was employed as a technique for the electrochemical characterization of each electrode surface. As such, the Nyquist plots for ACOP showed a significant difference in responses for all four electrodes, as shown in Fig. 3(a). In addition, a semicircle with a large diameter was observed for the PCPE in the frequency range 10^{-2}–10^{6} Hz. However, the diameter of the semicircle diminished when the ISSM-CNT-PE was employed. Furthermore, the charge transfer resistance (R_{ct}) values obtained from Fig. 3(a) for ACOP (5.0×10^{-5} M) at the PCPE, the ISSM-PE, the CNT-PE and the ISSM-CNT-PE were 235, 133, 122.5 and 65 kΩ, respectively. This observation implied that the charge transfer resistance of the electrode surface decreased and that the charge transfer rate increased upon employing the ISSM-CNT-PE. A Warburg at 45° was also observed for all the electrodes of interest.

Further electrochemical characterization of the electrode surface was performed using a Bode plot (Fig. 3(b)). In the absence of TX 100, only a single, symmetrical peak existed on the Bode plot of phase angle (Φ) vs. log frequency (f), which corresponded to the relaxation process of the electrode/solution interface, as given in Fig. 3(b). However, the Bode plot was very different when 5×10^{-5} M TX 100 was present, showing two well-defined peaks corresponding to the two relaxation processes, (I) and (II). The adsorption of surfactants on hydrophobic surfaces has been investigated previously, and a common observation was that, at high concentrations, surfactants usually form a monolayer on the electrode surface. Due to the suspected formation of this monolayer, the smoothness of the surface of the surfactant-modified electrodes increased in comparison to the unmodified ones.

Proceeding from very low concentrations (1×10^{-7} M) of surfactants to high concentrations (1×10^{-3} M), the adsorptive behavior of TX 100 on a hydrophobic surface changes from monomer adsorption to monolayer adsorption. As the relaxation of the electrolyte solution usually occurred at high frequencies, relaxation (I) on the curve was attributed to the electrolyte solution, and relaxation (II) was due to the monolayer of TX 100 on the electrode surface. It was interesting to note that, for those electrodes in which there was no surfactant present, the second relaxation was not observed. This result further verified the above-mentioned rea-

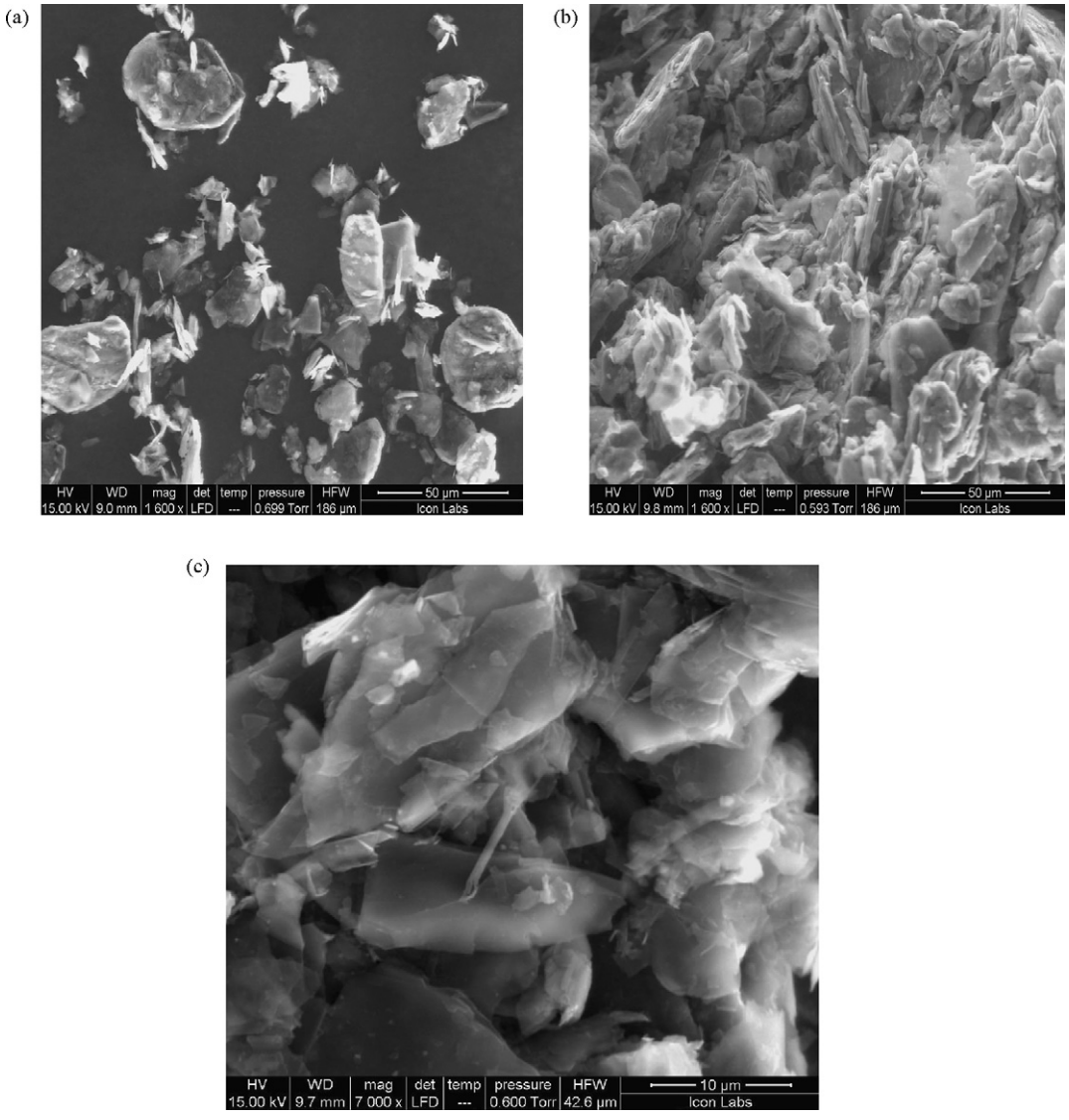

Fig. 1. Scanning electron microscope images of (a) PCPE, (b) ISSM-PE and (c) ISSM-CNT-PE.

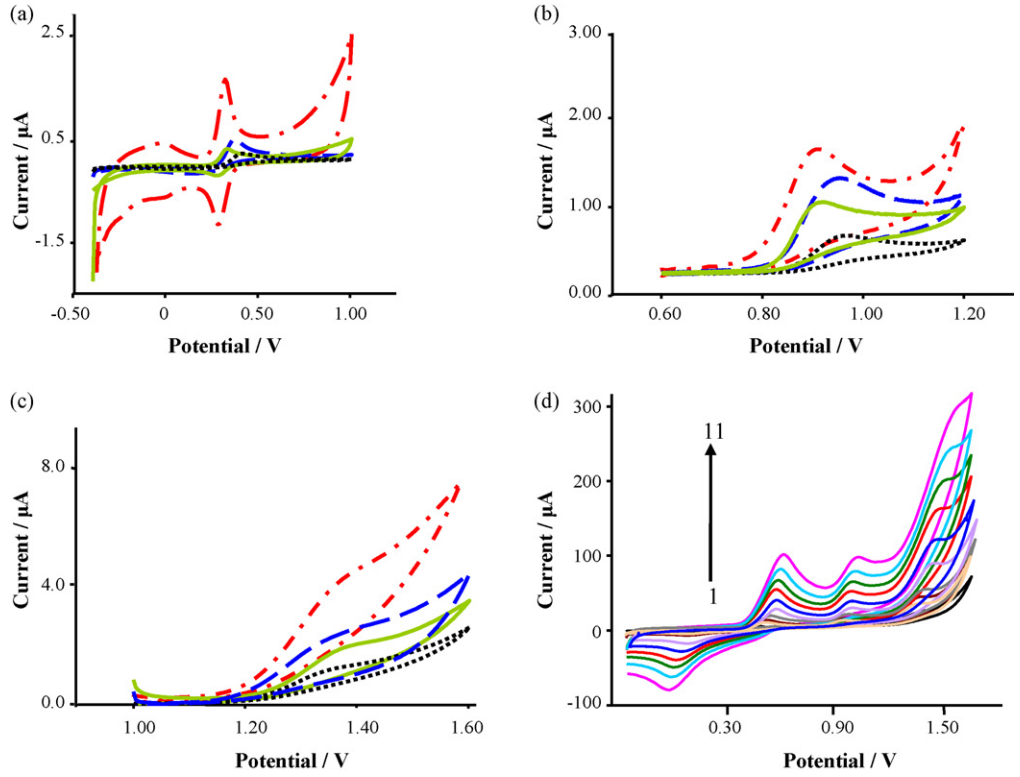

Fig. 2. Cyclic voltammograms of 1×10^{-6} M ACOP (a), ASA (b) and CF (c) at four different electrodes: PCPE (···), CNT-PE (– – –), ISSM-PCPE (—) and ISSM-CNT-PE (– · – · –). Voltammetric conditions: scanning electrode potential with a scan rate of 10 mV s^{-1} between −0.4 and +1.0 V for ACOP, +0.6–1.2 V for ASA and +1.0–1.6 V for CF in phosphate buffer solution (pH 7.0) containing 5.00×10^{-5} M TX 100. (d) Cyclic voltammograms of ACOP, ASA and CF (1.0×10^{-6} M) obtained simultaneously in phosphate buffer solution (pH 7.0) containing 5.00×10^{-5} M TX 100 employing varying scan rates (mV s^{-1}): (1–11) 100, 200, 300, 400, 500, 1000, 1500, 2000, 2500, 3000 and 3500.

sons of the process of formation of TX 100 layer onto the electrode surface. In addition, the ISSM-CNT-PE showed a lower relaxation than the ISSM-PE electrode, implying that the reaction was more facile on the former electrode. This conclusion was supported by another type of Bode plot that compared log$Z$ vs. log$f$. In the frequency range of relaxation (I), the dependence of log$Z$ vs. log$f$ gave a slope of −0.5, corresponding to the Warburg impedance associated with the electrolyte solution. As for relaxation (II), the slope for log$Z$ vs. log$f$ was −0.55, indicating the presence of a constant phase element in the relaxation of the TX 100 monolayer.

The dependence of log$Z$ on log$f$ in the absence of TX 100 had a slope of −0.8, corresponding to the capacitance of the electric double layer. A slope of almost zero at the two extremes represented the capacitance of the electric double layer as well as the two resistances associated with the electrolyte solution and the charge transfer between the solution and the electrode. As discussed above, the resistance of the electrolyte solution usually appeared at high frequencies; thus, the plateau at high frequencies on the Bode plane plots corresponded to the electrolyte solution resistance, and the plateau at low frequencies was associated with the charge transfer process. Similar results were obtained for ASA and CF employing all four electrodes.

Finally, the Kramers–Kronig transformation test was carried out on ACOP to test the validity of the impedance data (Fig. 3(c)). The Kramers–Kronig transformation gave a χ^2 (chi square) of 3.48×10^{-6} for ACOP, 7.85×10^{-6} for ASA and 6.69×10^{-6} for CF. Therefore, the system satisfied all the conditions for very good impedance data (i.e., linearity, causality, stability and finiteness of the system). Thus, the test implied that the impedance data were validated with respect to impedances over a wide frequency range and were of very good quality.

3.6. Chronocoulometry (CC)

Electro-oxidation of ACOP, ASA and CF at the PCPE, CNT-PE, ISSM-PE and ISSM-CNT-PE was characterized by employing chronocoulometry for the determination of the kinetics and mechanisms of electrode reactions. Using double potential step chronocoulometry, after point-by-point background subtraction, the plot of charge (Q) vs. the square root of time ($t^{1/2}$) showed a linear relationship. According to the integrated Cottrell equation, the diffusion coefficient and Q_{ads} of ACOP, ASA and CF could then be estimated from the slope and intercept, respectively, of the plot of total Q vs. $t^{1/2}$, given by the Anson equation [48]. The resulting calculated parameters are presented in Table S1. As can be observed from the data, the value of the slope and the Q_{ads} for the ISSM-CNT-PE were more than the other electrodes, confirming that TX 100, along with CNTs, makes the accumulation of ACOP, ASA and CF on the electrode surface more effective.

The surface coverage (Γ^0) for all four electrodes was calculated using the following relationship:

$$Q_{ads} = nFA\Gamma^0 \quad (1)$$

and the results are given in Table S1. From these values, it was observed that the surface coverage was maximum in the case of the ISSM-CNT-PE. Moreover, the diffusion coefficients (D) obtained in the micellar media was greater than the D obtained in aqueous media. Thus, due to the synergistic effect of CNTs and TX 100, the electrode surface coverage by ACOP, ASA and CF drastically increased and the kinetics of oxidation became more facile, thereby confirming the results obtained from CV.

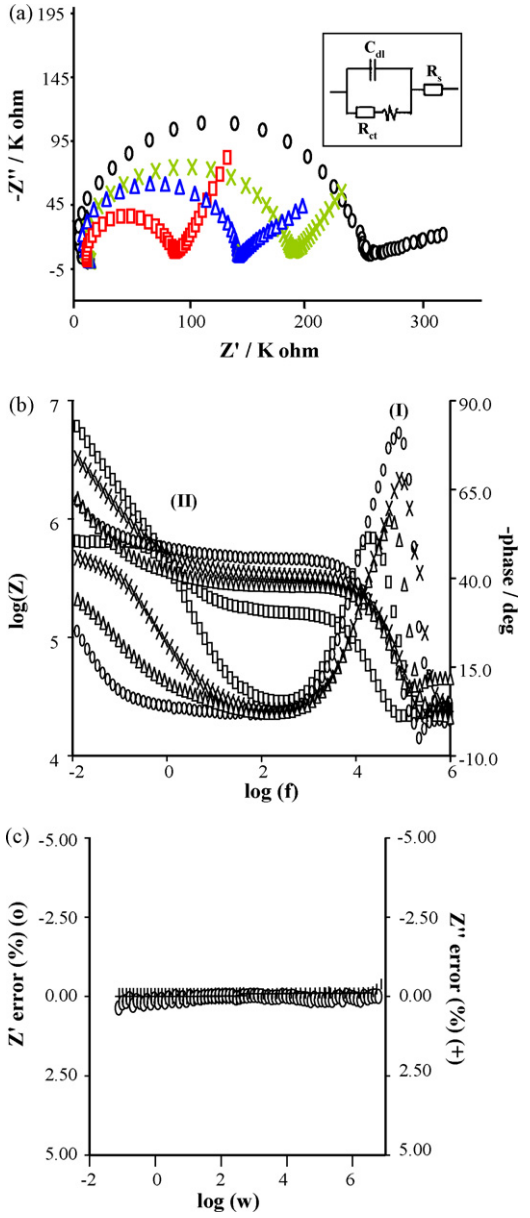

Fig. 3. (a) Nyquist plots for EIS measurements (5.0×10^{-5} M ACOP) at PCPE (○), ISSM-PE (×), CNT-PE (△) and ISSM-CNT-PE (□). In the box on the right upper side is the equivalent circuit used for data fitting. (b) Bode plots: (i) logarithmic plot of frequency vs. impedance and (ii) logarithmic plot of frequency vs. phase angle at the PCPE (○), the ISSM-PE (×), the CNT-PE (△) and the ISSM-CNT-PE (□). (c) Kramers–Kronig transformation test (plot of $\log\omega$ vs. error in Z^{I} or Z^{II}) for 5.0×10^{-5} M ACOP at the ISSM-CNT-PE in phosphate buffer solution (pH 7.0) containing 5.00×10^{-5} M TX 100. The amplitude of the perturbation was 10 mV and the frequency range was from 10^{-2} Hz to 10^{6} Hz.

3.7. Adsorptive stripping differential pulse voltammetry (AdSDPV)

AdSDPV was employed to study the influence of the accumulation potential (E_{acc}) and the accumulation time (t_{acc}) on the oxidation peak current of ACOP, ASA and CF in the presence of TX 100 (Fig. S4). Keeping the t_{acc} as 60 s, E_{acc} was determined by employing a potential window of −1.2 V to +0.5 V. The peak current for ACOP reached its maximum at an E_{acc} of −0.7 V (Fig. S4(a)), whereas that for ASA and CF occurred at −0.6 V (Fig. S4(b)) and at −0.4 V (Fig. S4(c)), respectively. Therefore, E_{acc} = −0.7 V was selected for all further studies. An increase in the accumulation time improved the sensitivity of determination. Hence, the effect of

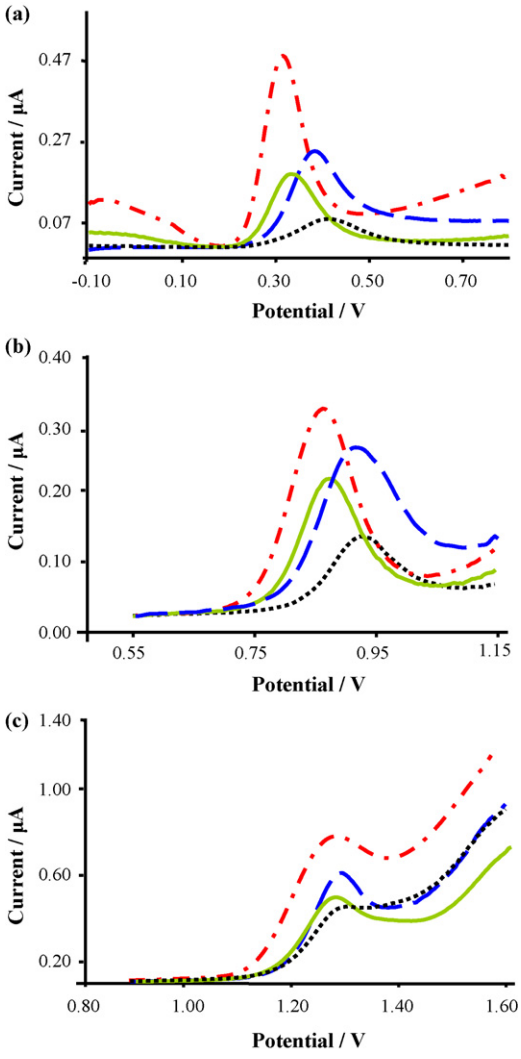

Fig. 4. AdSDPV of 8×10^{-7} M ACOP (a), ASA (b) and CF (c) at four different electrodes: PCPE (···), CNT-PE (– – –), ISSM-PCPE (—) and ISSM-CNT-PE (–·–·–). Voltammetric conditions: E_{acc} = −0.7 V, t_{acc} = 300 s, step potential = 5 mV and modulation amplitude = 50 mV in phosphate buffer solution (pH 7.0) containing 5.00×10^{-5} M TX 100.

the variation of t_{acc} was studied over a period of 10–600 s, keeping E_{acc} = −0.7 V constant at a concentration of 1.27×10^{-6} M. From 10 to 300 s, there was a linear increase in the peak current of ACOP and ASA (Fig. S4(a) and (b)). This same increase was seen in the range of 10–330 s for CF (Fig. S4(c)). Beyond this range, the current began to level off for the analytes of interest. This observation implied that surface saturation occurred at higher accumulation times. Thus, t_{acc} of 300 s was selected as the optimum time where all three analytes could be determined with good sensitivity.

A comparative study was also carried out, employing AdSDPV for 8×10^{-7} M ACOP, ASA and CF (Fig. 4) on the PCPE, the ISSM-PE, the CNT-PE and the ISSM-CNT-PE. From these experiments, it could be observed that the best results for both peak current and peak potential were obtained from the ISSM-CNT-PE. The resulting oxidation peak potentials obtained for ACOP, ASA and CF at the PCPE were 0.40, 0.94 and 1.30 V, respectively, whereas the peak potentials obtained at the ISSM-CNT-PE were 0.30, 0.85 and 1.27 V, respectively. Thus, it can be concluded that the electro-oxidation of all three molecules became facile at the ISSM-CNT-PE surface.

The oxidation products found were N-acetyl-p-quinone imine for acetaminophen [Scheme 1 , (1)], which involved two proton and two electron transfers [49], and 3,6-dioxocyclohexa-1,4-

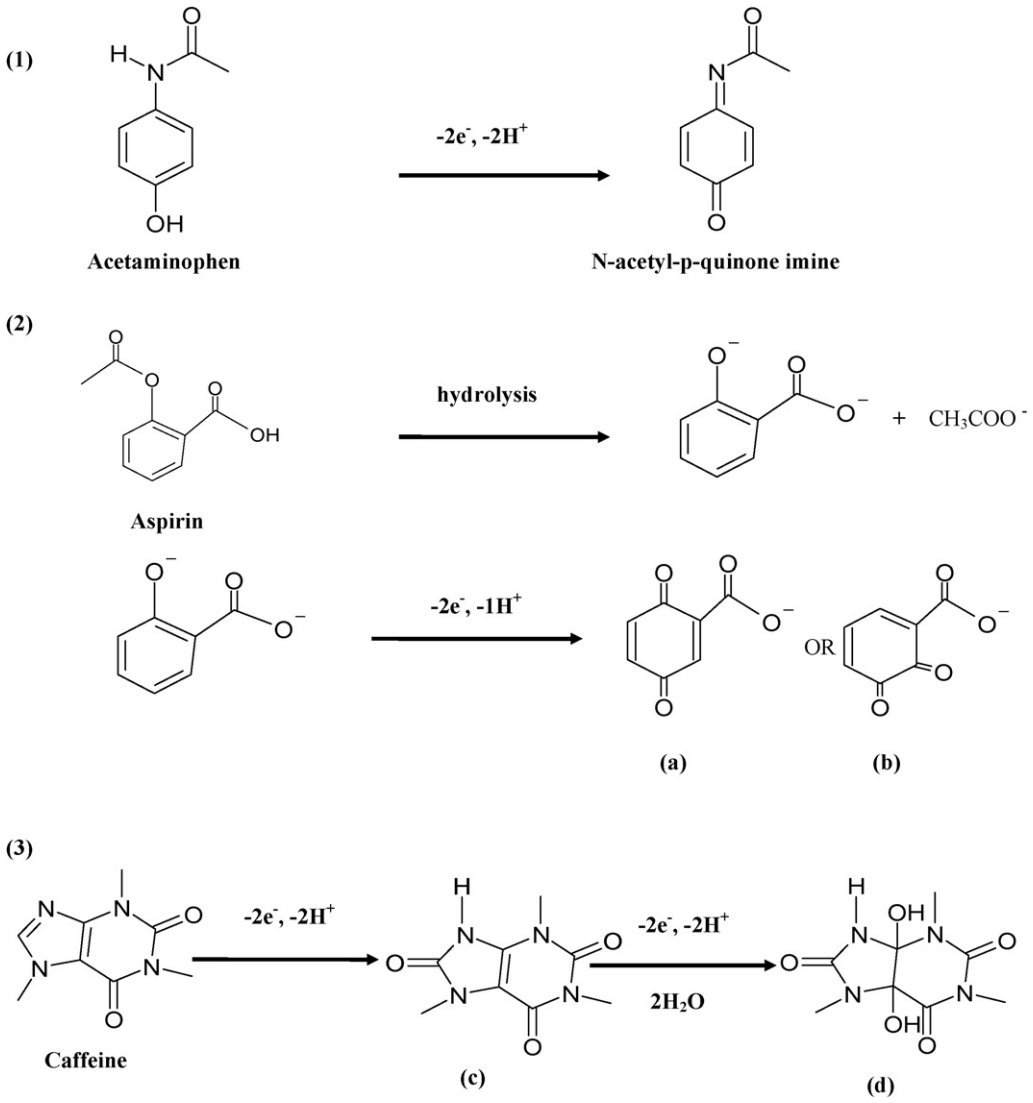

Scheme 1. Oxidation reactions for ACOP, ASA and CF.

Table 1
Analytical parameters for electrochemical determination of ACOP, ASA and CF in phosphate buffer solution at pH 7.0.

No.	Molecule	LWR	LRE	r	LOD	%RSD
(A) Statistical data for individual molecules						
1	ACOP	1.12×10^{-7}–6.94×10^{-5} M	I_p (μA) = $0.0771\times10^{-6}C$ (μM) + 0.350	0.9979	2.11×10^{-8} M	2.92
2	ASA	2.39×10^{-7}–6.45×10^{-5} M	I_p (μA) = $0.0654\times10^{-6}C$ (μM) + 0.2235	0.9965	7.51×10^{-8} M	1.58
3	CF	2.82×10^{-7}–6.61×10^{-5} M	I_p (μA) = $0.0608\times10^{-6}C$ (μM) + 0.162	0.9981	8.26×10^{-8} M	2.16
(B) Statistical data for two molecules simultaneously when the concentration of the third molecule is kept constant (8.00×10^{-7} M)						
5	ACOP	2.77×10^{-7}–6.40×10^{-5} M	I_p (μA) = $0.0741\times10^{-6}C$ (μM) + 0.2685	0.9977	2.46×10^{-8} M	2.54
6	ASA		I_p (μA) = $0.0598\times10^{-6}C$ (μM) + 0.2852	0.9963	8.37×10^{-8} M	1.82
7	ACOP	2.85×10^{-7}–6.43×10^{-5} M	I_p (μA) = $0.0545\times10^{-6}C$ (μM) + 0.1477	0.9984	2.28×10^{-8} M	2.32
8	CF		I_p (μA) = $0.0772\times10^{-6}C$ (μM) + 0.350	0.9948	8.69×10^{-8} M	2.51
9	ASA	2.81×10^{-7}–6.54×10^{-5} M	I_p (μA) = $0.0584\times10^{-6}C$ (μM) + 0.2108	0.9974	8.44×10^{-8} M	1.96
10	CF		I_p (μA) = $0.0528\times10^{-6}C$ (μM) + 0.2247	0.9972	8.73×10^{-8} M	2.38
(C) Statistical data for one molecule when the concentrations of the other two molecules are kept constant (8.00×10^{-7} M each)						
11	ACOP	1.43×10^{-7}–6.53×10^{-5} M	I_p (μA) = $0.0758\times10^{-6}C$ (μM) + 0.3114	0.9969	2.33×10^{-8} M	2.37
12	ASA	2.79×10^{-7}–6.45×10^{-5} M	I_p (μA) = $0.0622\times10^{-6}C$ (μM) + 0.2000	0.9937	8.17×10^{-8} M	1.82
13	CF	2.65×10^{-7}–6.49×10^{-5} M	I_p (μA) = $0.0572\times10^{-6}C$ (μM) + 0.1531	0.9954	8.43×10^{-8} M	2.48
(D) Statistical data for all the three molecules simultaneously						
14	ACOP	2.91×10^{-7}–6.27×10^{-5} M	I_p (μA) = $0.0785\times10^{-6}C$ (μM) + 0.2061	0.9942	2.58×10^{-8} M	3.34
15	ASA		I_p (μA) = $0.0637\times10^{-6}C$ (μM) + 0.2203	0.9949	8.47×10^{-8} M	2.61
16	CF		I_p (μA) = $0.0545\times10^{-6}C$ (μM) + 0.1249	0.9987	8.83×10^{-8} M	3.03

LWR: linear working range; RSD: relative standard deviation; LOD: limit of detection; LRE: linear regression equation; r: correlation coefficient.

dienecarboxylate (a) or 5,6-dioxocyclohexa-1,3-dienecarboxylate (b) for aspirin [Scheme 1, (2)], which involved two electron and one proton transfers [50]. The mechanism of CF [Scheme 1, (3)] electro-oxidation, however, involved four electrons and four protons. In this more complicated process, the first step was a two electron, two proton oxidation of the C-8–N-9 bond to give the substituted uric acid (c), followed by an immediate two electron and two proton electro-oxidation to the 4,5-diol analogue of uric acid (d), which rapidly fragmented [51,52].

3.8. Individual and simultaneous voltammetric determination of ACOP, ASA and CF

3.8.1. Determination of ACOP, ASA and CF individually

Based on the above findings, an analytical method was proposed for determining concentrations of ACOP, ASA and CF employing AdSDPV. The optimized conditions were applied for finding the limit of detection (LOD) (S/N = 3), the linear working range (LWR), the linear regression equation (LRE) and the correlation coefficient (r) (Table 1(A)).

3.8.2. Determination of ACOP, ASA and CF simultaneously

The proposed AdSDPV method was employed for the simultaneous determination of ACOP, ASA and CF in synthetic samples. In this respect, three separate cases were studied. In the first case, the concentration of one molecule was increased linearly in the presence of fixed concentrations of the other two (Fig. 5(a)). In the second case, the concentrations of two molecules were increased simultaneously while keeping the concentration of the third constant (Fig. 5(b)). For the third case, the three molecules were determined when simultaneously increasing their concentrations (Fig. 6). The statistical results for the above three cases are summarized in Table 1(B)–(D).

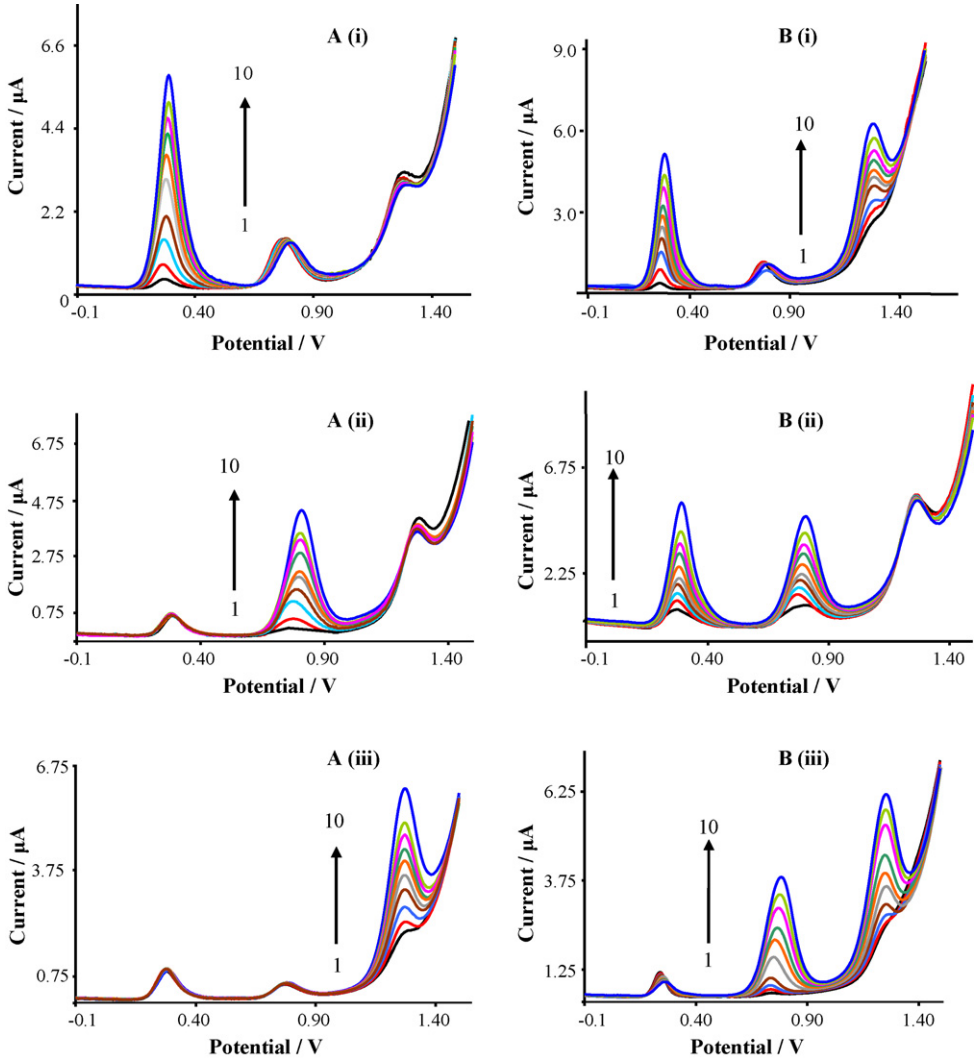

Fig. 5. (A) (i) AdSDPV curves obtained at the ISSM-CNT-PE for ACOP at different concentrations in the presence of 5×10^{-6} M ASA and CF: (1) 1.43×10^{-7}, (2) 2.42×10^{-6}, (3) 4.33×10^{-6}, (4) 9.78×10^{-6}, (5) 1.58×10^{-5}, (6) 2.19×10^{-5}, (7) 3.29×10^{-5}, (8) 4.14×10^{-5}, (9) 5.32×10^{-5} and (10) 6.53×10^{-5} M. (ii) AdSDPV curves obtained at the ISSM-CNT-PE for ASA at different concentrations in the presence of 4.14×10^{-6} M ACOP and CF: (1) 2.8×10^{-7}, (2) 2.41×10^{-6}, (3) 4.89×10^{-6}, (4) 6.87×10^{-6}, (5) 1.10×10^{-5}, (6) 1.89×10^{-5}, (7) 3.11×10^{-5}, (8) 4.52×10^{-5}, (9) 5.34×10^{-5} and (10) 6.42×10^{-5} M. (iii) AdSDPV curves obtained at the ISSM-CNT-PE for CF at different concentrations in the presence of 4.2×10^{-5} M ACOP and ASA: (1) 0.27×10^{-7}, (2) 2.73×10^{-6}, (3) 5.10×10^{-6}, (4) 7.39×10^{-6}, (5) 1.28×10^{-5}, (6) 2.01×10^{-5}, (7) 3.26×10^{-5}, (8) 4.74×10^{-5}, (9) 5.43×10^{-5} and (10) 6.50×10^{-5} M. (B) (i) AdSDPV curves obtained at the ISSM-CNT-PE for ACOP and CF at different concentrations in the presence of 3.9×10^{-6} M ASA: (1) 2.85×10^{-7}, (2) 2.89×10^{-6}, (3) 3.72×10^{-6}, (4) 5.51×10^{-6}, (5) 1.03×10^{-6}, (6) 1.89×10^{-6}, (7) 2.99×10^{-5}, (8) 3.91×10^{-5}, (9) 5.44×10^{-5} and (10) 6.43×10^{-5} M. (ii) AdSDPV curves obtained at the ISSM-CNT-PE for ACOP and ASA at different concentrations in the presence of 2.5×10^{-5} M CF: (1) 2.77×10^{-7}, (2) 3.75×10^{-6}, (3) 8.72×10^{-6}, (4) 1.55×10^{-5}, (5) 2.25×10^{-5}, (6) 2.79×10^{-5}, (7) 3.19×10^{-5}, (8) 4.18×10^{-5}, (9) 5.31×10^{-5} and (10) 6.40×10^{-5} M. (iii) AdSDPV curves obtained at the ISSM-CNT-PE for ASA and CF at different concentrations in the presence of 5×10^{-6} M ACOP: (1) 2.81×10^{-7}, (2) 2.83×10^{-6}, (3) 3.97×10^{-6}, (4) 6.82×10^{-6}, (5) 1.28×10^{-5}, (6) 2.04×10^{-5}, (7) 3.21×10^{-5}, (8) 4.19×10^{-5}, (9) 5.27×10^{-5} and (10) 6.48×10^{-5} M. Other conditions were as in Fig. 3.

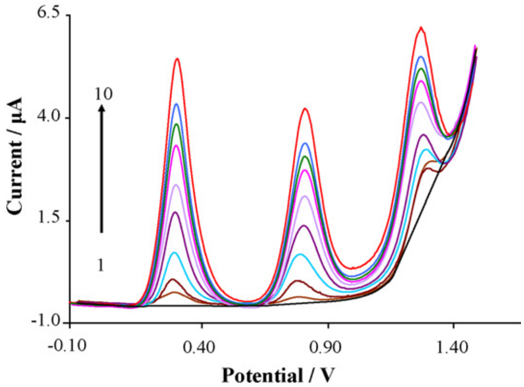

Fig. 6. AdSDPV curves obtained for the oxidation of ACOP, ASA and CF at equal concentrations of each: (1) blank, (2) 2.91×10^{-7}, (3) 2.89×10^{-6}, (4) 7.62×10^{-6}, (5) 1.78×10^{-5}, (6) 2.56×10^{-5}, (7) 3.10×10^{-5}, (8) 4.08×10^{-5}, (9) 5.32×10^{-5} and (10) 6.27×10^{-5} M. Other conditions were as in Fig. 3.

The LOD and LWR obtained in all of the aforementioned cases matched well with the case when the three molecules were analyzed individually. Thus, it could be concluded that, by employing the proposed AdSDPV method, the simultaneous determination of all three molecules was as efficient as their individual determinations.

3.9. Interference studies, validation studies and analytical applications

Under optimal experimental conditions, the interference from selected metal ions and organic compounds was evaluated. The tolerance limit for interfering species was considered as the maximum concentration that gave a relative error less than ± 5.0% at a concentration of 8.0×10^{-7} M of ACOP. Phenol, ascorbic acid, caffeine, uric acid, glucose and 4-aminophenol were the most common constituents found with ACOP. From the studies, a 80-fold excess of ascorbic acid had no effect on the i_p of ACOP (Fig. S5). Glucose, uric acid, citric acid and urea also did not interfere until a 100-fold excess was achieved. In addition, 4-aminophenol showed no changes in i_p until a 70-fold excess was used. Even a 200-fold excess of K^+, Ca^{2+}, NO_3^-, NH_4^+, Cl^- or Mg^{2+} had no effect on the i_p of ACOP, ASA or CF. These results suggested that the determination of all three molecules in pharmaceutical formulations and biological samples at an ISSM-CNT-PE was not significantly affected by the most common interfering species.

For validation of the proposed method, various parameters, such as repeatability, reproducibility, precision and accuracy of analysis, were obtained by performing five replicate measurements for 1.51×10^{-6} M standard ACOP, 1.38×10^{-6} M standard ASA, and 1.94×10^{-6} M standard CF over a single day (intraday assay, $n = 5$) and for 5 days over a period of 1 week (interday assay). Satisfactory mean percentage recoveries (%*R*) and relative standard deviations (% RSD) were obtained and are reported in Table S2(a). The recoveries obtained confirmed both the high precision of the proposed procedure and the stability of ACOP, ASA and CF solutions.

The robustness of the proposed procedure [Table S2(b)] was also examined by studying the effect of small variations in pH (6.5–7.5), accumulation potential E_{acc} (−0.60 to −0.80 V) and accumulation time (250–350 s) on the recovery of ACOP, ASA and CF. As can be seen from Table S2, %*R* for the three molecules were in the range of 98–102% under all variable conditions and did not show a significant change when the critical parameters were varied; hence, the method was robust in nature.

For further evaluation of the validity of the proposed method, recovery tests for ACOP, ASA and CF in pharmaceutical for-

Table 2
Comparison between the proposed method and the Indian Pharmacopoeia method for sample analysis.

Sample	ACOP			ASA			CF		
	a	*b*	*c*	*a*	*b*	*c*	*a*	*b*	*c*
Crocin	500	497.7 ± 1.2	492.7 ± 1.7	–	–	–	–	–	–
Calpol	500	489.4 ± 0.9	506.6 ± 1.5	–	–	–	–	–	–
Paracip 100	100	099.2 ± 1.4	098.9 ± 2.5	–	–	–	–	–	–
Anacin	500	487.3 ± 1.9	496.3 ± 2.3	–	–	–	30	29.9 ± 1.8	29.8 ± 3.0
Disprin	–	–	–	350	348.9 ± 2.2	343.61 ± 2.7	–	–	–
Bayer aspirin	–	–	–	300	299.6 ± 1.6	294.35 ± 1.9	–	–	–
Coffee sample (espresso)	–	–	–	–	–	–	90.00 (per 2 fl. oz.)	89.2 ± 1.9	87.3 ± 2.6
Coffee sample (instant)	–	–	–	–	–	–	65.00[a]	64.3 ± 1.4	62.8 ± 2.2
Cola beverage sample	–	–	–	–	–	–	35.00[a]	34.8 ± 0.9	32.7 ± 1.5
Cola beverage sample	–	–	–	–	–	–	36.50[a]	36.0 ± 1.3	35.3 ± 1.9
Synthetic sample 1	200	201.8 ± 0.6	197.7 ± 1.1	300	298.9 ± 1.8	297.7 ± 2.9	45	46.9 ± 1.4	42.8 ± 1.5
Synthetic sample 2	250	249.3 ± 1.9	246.6 ± 2.8	220	219.1 ± 1.3	218.6 ± 2.1	60	61.1 ± 1.2	56.7 ± 1.3
Cipstrong tablet	125	126.6 ± 1.3	123.7 ± 1.8	325	325.7 ± 1.1	322.4 ± 1.4	30	29.6 ± 1.9	27.2 ± 2.5

a: amount (mg) of drug in the sample; *b*: amount (mg) of drug obtained by the proposed method ± %RSD ($n = 5$); *c*: amount (mg) of drug obtained by the standard method ± %RSD ($n = 5$).
[a] Per 8 fl. oz.

Table 3
Comparison between various electroanalytical methods for the individual determination of ACOP, ASA and CF with the proposed method.

Molecule	Modified electrodes	Linear working range (M)	Limit of detection (M)	Samples analyzed	References
ACOP	MWCNT modified basal plane pyrolytic graphite electrode	1.0×10^{-8}–2.0×10^{-6}	1.00×10^{-8}	Pharmaceutical formulations	[1]
	Palladium nanocluster – coated polyfuran	5.0×10^{-7}–10×10^{-5}	7.64×10^{-8}	–	[2]
	Graphene modified glassy carbon electrode	1.0×10^{-7}–2.0×10^{-5}	3.20×10^{-8}	Pharmaceutical formulations	[3]
	Thionine immobilized MWCNT modified CPE	1.0×10^{-7}–10×10^{-5}	5.00×10^{-8}	Blood plasma samples	[4]
	Boron doped diamond electrode	6.0×10^{-7}–8.3×10^{-5}	4.60×10^{-7}	Pharmaceutical formulations	[5]
	ISSM-CNT-PE	1.12×10^{-7}–6.94×10^{-5}	2.58×10^{-8}	Pharmaceutical formulations, urine and blood serum samples	This work
ASA	Boron doped diamond electrode	2.50×10^{-6}–1.05×10^{-4}	2.0×10^{-6}	Pharmaceutical formulations	[8]
	Nickel hydroxide modified nickel electrode	2.0×10^{-4}–7.0×10^{-3}	4.8×10^{-5}	Pharmaceutical formulations	[9]
	Cobalt hydroxide modified glassy carbon electrode	5.0×10^{-5}–5.5×10^{-4}	1.88×10^{-6}	Urine sample	[48]
	ISSM-CNT-PE	2.39×10^{-7}–6.45×10^{-5}	8.47×10^{-8}	Pharmaceutical formulations, urine and blood serum samples	This work
CF	Boron doped diamond electrode	3.0×10^{-7}–9.1×10^{-5}	1.47×10^{-7}	Pharmaceutical formulations	[5]
	Nafion coated glassy carbon electrode	9.95×10^{-7}–1.06×10^{-5}	7.98×10^{-7}	Cola beverages	[11]
	1,4-Benzoquinone modified carbon paste electrode	5.0×10^{-4}–8.0×10^{-3}	5.1×10^{-6}	Coffee samples	[13]
	Nafion–ruthenium oxide pyrochlore CME	5.0×10^{-6}–2.0×10^{-4}	2.0×10^{-6}	Coffee and cola beverages	[14]
	ISSM-CNT-PE	2.82×10^{-7}–6.61×10^{-5}	8.83×10^{-8}	Pharmaceutical formulations, cola and coffee beverages, urine and blood serum samples	This work

mulations, urine and human serum samples were carried out. Unfortunately, we could obtain only one pharmaceutical formulation, which contained a combination of ACOP, ASA and CF; hence, recovery tests were performed on synthetic mixtures, as mentioned in Table S3. These tests gave %*R* values in the range of 98.0–102% for all three molecules. Similarly, recovery tests were performed on morning urine samples collected from healthy volunteers. The %*R* obtained for these samples were in the range of 96.5–98.5% for all three molecules, detected simultaneously.

Additionally, recovery tests were also performed on human blood serum. However, proteins are known to be repelled by non-ionic surfactants that contain a polyethylene glycol (PEG) group. Even though TX 100 has 9.5 ethylene oxide units on average, which is less than common PEG, some repelling effect was still expected. Fortunately, when a highly diluted serum sample solution was taken for analysis, the fouling effect on the electrode surface was found to be negligible. The %*R* obtained in this case was then in the range of 98.5–103.0% (Table S3). Recovery tests for CF were also carried out in decaffeinated cola and coffee samples, and the %*R* values obtained were in the range of 98.7–101.5%.

Based on these results, recovery results were not affected significantly, and consequently, the described method was accurate for the assay of ACOP, ASA and CF in complex matrices. For analytical applications, the determination of the amount of ACOP, ASA and CF in all samples have been carried out by the standard addition method. The amount of ACOP, ASA and CF obtained in the pharmaceutical formulations and caffeinated beverages by the proposed method was found to agree well with the label contents. The results also showed that interferences from the matrix were negligible.

Simultaneous determination of all three molecules of interest was carried out in pharmaceutical formulations in the same manner as for the individual samples. The proposed method was further validated by employing UV–vis spectrophotometry for ACOP, potentiometry for CF and titrimetry for ASA, as proposed in the Indian Pharmacopoeia [53]; the results are given in Table 2. This table shows that the amounts of ACOP, ASA and CF obtained by the proposed method agreed well with the amount obtained by the standard methods. Applying a paired *t*-test to the results obtained by this procedure and those claimed on the labels, it was found that all results were in agreement at the 95% confidence level and within an acceptable range of error. Thus, individual and simultaneous determination of ACOP, ASA and CF can be carried out with great confidence in various matrices by the proposed method.

A comparison between the analytical performance of the present method and some previous literature methods for the determination of ACOP, ASA and CF are given in Table 3. The lowest limit of detection (1.00×10^{-8} M) obtained for the determination of ACOP was by an MWCNT modified Basal plane pyrolytic graphite electrode (MWCNT-BPPGE) (4.9 mm diameter) [1]. In comparison, the ISSM-CNT-PE employed in the present work has a diameter of 0.5 mm, which is about 10-times smaller than this previously used electrode [1]. Moreover, MWCNT-BPPGE has been employed for the analysis of ACOP only in pharmaceutical formulations without simultaneous determination of any major interfering components present in real samples. However, the proposed electrode has already been employed for the simultaneous determination of ACOP, ASA and CF in pharmaceutical formulations, urine and blood serum samples. Furthermore, the limits of detection obtained for ASA and CF were the lowest by the proposed method, as shown in Table 3. These results reveal that the proposed ISSM-CNT-PE has a large advantage over other proposed methods in terms of linear working range, limit of detection and number of analyzed samples, in addition to the novel, simultaneous determination of ACOP, ASA and CF in a complex matrix.

4. Conclusion

The results obtained in the paper demonstrate the synergistic effect of TX 100 and an MWCNT modified carbon paste electrode on the first simultaneous voltammetric determination of ACOP, ASA and CF. Additionally, the oxidation peak currents of the three molecules were observed to remarkably increase at the ISSM-CNT-PE surface. Moreover, the proposed method was very sensitive, free of common interferences with the molecules of interest and had sub-micromolar detection limits. This method can be employed for the simultaneous determination of the three molecules of interest in pharmaceutical formulations, urine and blood serum samples. Consequently, this method is recommended for both the individ-

ual and the simultaneous determination of all three molecules at trace levels in clinical and quality control laboratories.

Acknowledgements

This research was partly funded by the University Grants Commission, New Delhi, India and by the US Army International Technology Center, Tokyo, Japan. We are thankful to Dr. M. Sudersanan for his kind help and suggestions. Thanks are also due to Prof. D.C. Kothari for providing kind help in obtaining SEM images from Icon Analytical.

Appendix A. Supplementary data

Supplementary data associated with this article can be found, in the online version, at doi:10.1016/j.electacta.2010.07.093.

References

[1] R.T. Kachoosangi, G.G. Wildgoose, R.G. Compton, Anal. Chim. Acta 618 (2008) 54.
[2] N.F. Atta, M.F. El-Kady, A. Galal, Sens. Actuators B 141 (2009) 566.
[3] X. Kang, J. Wang, H. Wu, J. Liu, I.A. Aksay, Y. Lin, Talanta 81 (2010) 754.
[4] S. Shahrokhian, E. Asadian, Electrochim. Acta 55 (2010) 666.
[5] B.C. Lourenção, R.A. Medeiros, R.C. Rocha-Filho, L.H. Mazo, O. Fatibello-Filho, Talanta 78 (2009) 748.
[6] P. Fanjul-Bolado, P.J. Lamas-Ardisana, D. Hernández-Santos, A. Costa-García, Anal. Chim. Acta 638 (2009) 133.
[7] C. Batchelor-McAuley, G.G. Wildgoose, Electrochem. Commun. 10 (2008).
[8] E.R. Sartori, R.A. Medeiros, R.C. Rocha-Filho, O. Fatibello-Filho, J. Braz. Chem. Soc. 20 (2009) 360.
[9] S. Majdi, A. Jabbari, H. Heli, J. Solid State Electrochem. 11 (2007) 601.
[10] O.-W. Lau, S.-F. Luk, Y.-M. Cheung, Analyst 114 (1989) 1047.
[11] B. Brunetti, E. Desimoni, P. Casati, Electroanalysis 19 (2007) 385.
[12] J.-M. Zen, Y.-S. Ting, Anal. Chim. Acta 342 (1997) 175.
[13] M. Aklilu, M. Tessema, M. Redi-Abshiro, Talanta 76 (2008) 742.
[14] J.-M. Zen, Y.-S. Ting, Y. Shih, Analyst 123 (1998) 1145.
[15] M. Barfield, N. Spooner, R. Lad, S. Parry, S. Fowles, J. Chromatogr. B 870 (2008) 32.
[16] M.J. Gomez, A. Agueera, M. Mezcu, J. Hurtado, F. Mocholi, A.R. Fernandez-Alba, Talanta 73 (2007) 314.
[17] M.A. Oliva, R.A. Olsina, A.N. Masi, Talanta 66 (2005) 229.
[18] K.K. Verma, A. Jain, Anal. Chem. 58 (1986) 821.
[19] A.B. Moreira, I.L.T. Dias, G.O. Neto, E.A.G. Zagatto, L.T. Kubota, Anal. Chim. Acta 523 (2004) 49.
[20] M.O. Iwunze, Anal. Lett. 41 (2008) 2944.
[21] S.S. Verenitch, A. Mazumder, Anal. Bioanal. Chem. 391 (2008) 2635.
[22] R. Injac, B. Srdjenovic, M. Prijatelj, M. Boskovic, K. Karljikovic-Rajic, B. Strukelj, J. Chromatogr. Sci. 46 (2008) 137.
[23] Y. Yamauchi, A. Nakamura, I. Kohno, K. Hatanaka, M. Kitai, T. Tanimoto, J. Chromatogr. A 1177 (2008) 190.
[24] J.C.L. Alves, R.J. Poppi, Anal. Chim. Acta 642 (2009) 212.
[25] Á.Z. Dávid, E. Mincsovics, I. Antal, É. Furdyga, Z. Zsigmond, I. Klebovich, J. Planar. Chromatogr.-Mod. TLC 19 (2006) 355.
[26] E. Dinç, A. Özdemir, D. Baleanu, Talanta 65 (2005) 36.
[27] M.M. Sena, R.J. Poppi, J. Pharm. Biomed. Anal. 34 (2004) 27.
[28] V.D. Vaze, A.K. Srivastava, Electrochim. Acta 53 (2007) 1713.
[29] R.R. Gaichore, A.K. Srivastava, Anal. Lett. 43 (2010) 1933.
[30] S.M. Mobin, B.J. Sanghavi, A.K. Srivastava, P. Mathur, G.K. Lahiri, Anal. Chem. 82 (2010) 5983.
[31] W.Z. Inês Rosane de Oliveira, M. Renata El-Hage de Barros Osório, A. Neves, I.C. Vieira, Sens. Actuators B 122 (2007) 89.
[32] S. Shahrokhian, M. Ghalkhani, M.K. Amini, Sens. Actuators B 137 (2009) 669.
[33] G.A. Rivas, M.D. Rubianes, M.L. Pedano, N.F. Ferreyra, G.L. Luque, M.C. Rodríguez, S.A. Miscoria, Electroanalysis 19 (2007) 823.
[34] T. Yang, N. Zhou, Y. Zhang, W. Zhang, K. Jiao, G. Li, Biosens. Bioelectron. 24 (2009) 2165.
[35] H. Dai, Y. Wang, X. Wu, L. Zhang, G. Chen, Biosens. Bioelectron. 24 (2009) 1230.
[36] H. Beitollahi, H. Karimi-Maleh, H. Khabazzadeh, Anal. Chem. 80 (2008) 9848.
[37] S. Zhu, L. Fan, X. Liu, L. Shi, H. Li, S. Han, G. Xu, Electrochem. Commun. 10 (2008) 695.
[38] I. Svancara, K. Vytras, K. Kalcher, A. Walcarius, J. Wang, Electroanalysis 21 (2008) 7.
[39] V.G. Gavalas, S.A. Law, J.C. Ball, R. Andrews, L.G. Bachas, Anal. Biochem. 329 (2004) 247.
[40] R. Jain, R. Mishra, A. Dwivedi, Colloids Surf. A 337 (2009) 74.
[41] S. Zhang, K. Wu, S. Hu, Talanta 58 (2002) 747.
[42] C. Li, Bioelectrochemistry 70 (2007) 263.
[43] Y. Xu, C. Hu, S. Hu, Bioelectrochemistry 74 (2009) 254.
[44] F. Valentini, A. Amine, S. Orlanducci, M.L. Terranova, G. Palleschi, Anal. Chem. 75 (2003) 5413.
[45] N.R. Martos, Diaz, L.F. Navalon, L.F. Capitan-Vallvey, Anal. Lett. 34 (2001) 579.
[46] A.K. Sanyal, A. Dutta, J. AOAC Int. 79 (1996) 1303.
[47] W. Guo, Anal. Lett. 32 (1999) 2335.
[48] F.C. Anson, Anal. Chem. 38 (1966) 54.
[49] D.J. Miner, J.R. Rice, R.M. Riggin, P.T. Kissinger, Anal. Chem. 53 (1981) 2258.
[50] M. Houshmand, A. Jabbari, H. Heli, M. Hajjizadeh, A.A. Moosavi-Movahedi, J. Solid State Electrochem. 12 (2008) 1117.
[51] N. Spataru, B.V. Sarada, D.A. Tryk, A. Fujishima, Electroanalysis 14 (2002) 721.
[52] B.H. Hansen, G. Dryhurst, J. Electroanal. Chem. 30 (1971) 407.
[53] Indian Pharmacopoeia, 1996, pp. 70, 122, 556.